

Chapter 12

Theory of Power Spectral Density and Feynman-Alpha Method in Accelerator-Driven System and Their Higher-Order Mode Effects

Toshihiro Yamamoto

Abstract This chapter discusses the theory of higher-order modes in the Feynman Y function and cross-power spectral density (CPSD) in an accelerator-driven system (ADS) where pulsed spallation neutrons are injected at a constant time interval. Theoretical formulae that consider the higher-order modes of the correlated and uncorrelated components in the Feynman Y function and CPSD for an ADS were recently derived in a paper published by the author. These formulae for the Feynman Y function and CPSD are applied to a subcritical multiplying system with a one-dimensional infinite slab geometry in this chapter. The Feynman Y functions and CPSD calculated with the theoretical formulae are compared with the Monte Carlo simulations of these noise techniques. The theoretical formulae reproduce the Monte Carlo simulations very well, thereby substantiating the theoretical formulae derived in this chapter. The correlated and uncorrelated components of the Feynman Y functions and CPSD are decomposed into the sum of the fundamental mode and higher-order modes. This chapter discusses the effect of subcriticality on the higher-order mode effects.

Keywords ADS • Feynman- α method • Higher-order mode • Monte Carlo • Neutron noise • Power spectral density

12.1 Introduction

In accelerator-driven systems (ADS), fission chain reactions are driven by spallation neutrons emitted from a proton beam target. An ADS is quite different from an ordinary nuclear reactor in that it is always operated at a subcritical state. Thus, the safety requirements for reactivity control can be eased in ADSs. The

T. Yamamoto (✉)

Kyoto University, Research Reactor Institute, 2-1010 Asashiro Nishi,
Kumatori-cho, Sennan-gun, Osaka 590-0494, Japan
e-mail: tyama@rri.kyoto-u.ac.jp

subcriticality of an ADS, however, needs to be continuously monitored to maintain its criticality safety. A reactor noise technique such as the Feynman- α method and the power spectral density method can be a potential candidate for monitoring the subcriticality of ADSs. The noise theory in ADSs is different from the classical reactor noise theory in that multiple neutrons are injected from the proton beam target at a single spallation event and pulsed neutrons are emitted deterministically at a constant period. Many theoretical and experimental studies on the noise theory in ADSs have been performed thus far. The theoretical formula for the Feynman- α method or Rossi- α method in ADSs was studied by, for example, Pázsit et al. [1], Pázsit et al. [2], Kitamura et al. [3], and Muñoz-Cobo et al. [4]. Another technique that uses the auto-power spectral density (APSD) or cross-power spectral density (CPSD) was studied by, for example, Muñoz-Cobo et al. [5], Rugama et al. [6], Ballester and Muñoz-Cobo [7], and Degweker and Rana [8]. Sakon et al. recently carried out a series of power spectral analyses in a thermal subcritical reactor system driven by a periodically pulsed 14 MeV neutron source at the Kyoto University Critical Assembly (KUCA) [9].

Both the Feynman- α method and the power spectral density method are intended to measure a prompt neutron time-decay constant α of the fundamental mode because the subcriticality is directly related to the fundamental mode α . The measured results, however, are inevitably contaminated by the higher-order mode components. To obtain an accurate knowledge of the subcriticality, the effect of the higher-order modes needs to be quantified in detail.

Endo et al. [10] derived a theoretical formula of the Feynman Y function that considers the higher order modes. Muñoz-Cobo et al. [11] also derived a similar theoretical formula from a different approach. Using these formulae, Yamamoto [12, 13] demonstrated quantitative analyses of the spatial- and energy-higher order modes in Feynman Y functions, respectively. In these two works, the Feynman Y functions were successfully resolved into spatial- or energy-higher order modes. These discussions, however, involved subcritical multiplying systems driven by a neutron source with Poisson character. They did not account for either a periodically pulsed neutron source or its non-Poisson character. Some previous work that considered the higher-order modes in the noise techniques for ADSs has been published (e.g., [6], [7]). In these previous publications, however, the effects of the higher-order modes have not been quantitatively investigated. Yamamoto [14, 15] presented the formulae of the Feynman Y function and CPSD for ADSs that consider the higher-order mode effects. Yamamoto [15] resolved the Feynman Y functions and power spectral densities into the mode components. Verification of the formulae was demonstrated by comparing the theoretical predictions with the Monte Carlo simulations of the subcriticality measurement in an ADS.

The purpose of the present chapter is to investigate how the subcriticality would affect Feynman Y function and power spectral density. The subcriticality of an ADS differs from design to design. The smaller the subcriticality, the larger the neutron multiplication that can be gained, which, on the other hand, decreases the margin of criticality safety. The subcriticality undergoes a gradual change as the fuel burn-up proceeds. The Feynman Y function and power spectral density emerge differently as

the subcriticality changes. This chapter shows the dependence of subcriticality measurement on its subcriticality, which will contribute to the design of ADSs and planning of subcriticality measurements in the future.

12.2 Theory of Feynman- α Method in ADS

This section reviews the theory on the higher-order modes in the Feynman- α method in an ADS based on the work of Yamamoto [15]. Neglecting the energy- and spatial dependence of neutrons in a subcritical system driven by a neutron source with Poisson character, we obtain the Feynman Y function (the variance-to-mean ratio of neutron counts minus unity) as

$$Y(\Delta) = \frac{\langle C_1(\Delta)C_1(\Delta) \rangle - \langle C_1(\Delta) \rangle^2}{\langle C_1(\Delta) \rangle} - 1 \propto \left(1 - \frac{1 - e^{-\alpha_0\Delta}}{\alpha_0\Delta} \right) \quad (12.1)$$

where Δ = counting gate width, $C_1(\Delta)$ = neutron counts in Δ , α_0 = fundamental mode prompt neutron time-decay constant. When considering the energy and spatial dependence in an ADS, however, the Feynman Y function is more involved, as shown next.

The formula for the Feynman Y function in an ADS where q spallation neutrons are emitted from the beam target at a constant period T is given by this expression [15]:

$$Y(\Delta) = \frac{\langle C_1(\Delta)C_1(\Delta) \rangle - \langle C_1(\Delta) \rangle^2}{\langle C_1(\Delta) \rangle} - 1 = Y_C(\Delta) + Y_{CS}(\Delta) + Y_{UN}(\Delta), \quad (12.2)$$

where

$$Y_C(\Delta) = \frac{2}{C_R} \sum_{\ell=0}^{\infty} \sum_{m=0}^{\infty} \sum_{n=0}^{\infty} \frac{S_{\ell} F_{\ell \rightarrow mn} D_{1,m} D_{1,n}}{\alpha_{\ell} (\alpha_m + \alpha_n) \alpha_n} \left(1 - \frac{1 - e^{-\alpha_n \Delta}}{\alpha_n \Delta} \right), \quad (12.3)$$

$$Y_{CS}(\Delta) = -\frac{2q}{C_R T} \sum_{m=0}^{\infty} \sum_{n=0}^{\infty} \frac{D_{1,m} D_{1,n} \Psi_m^* \Psi_n^*}{(\alpha_m + \alpha_n) \alpha_n} \left(1 - \frac{1 - e^{-\alpha_n \Delta}}{\alpha_n \Delta} \right), \quad (12.4)$$

$$Y_{UN}(\Delta) = \frac{4q^2}{C_R \Delta T^2} \sum_{n=0}^{\infty} \sum_{\ell=0}^{\infty} \sum_{m=1}^{\infty} D_{1,n} D_{1,\ell} \Psi_n^* \Psi_{\ell}^* \frac{A_{\ell mn} (1 - \cos(\omega_m \Delta))}{\omega_m^2 (A_{\ell mn}^2 + B_{\ell mn}^2)}, \quad (12.5)$$

the angle brackets denote the ensemble-averaging operator, C_R = count rate, and α_m = time-decay constant of the m^{th} -order mode. (Refer to Yamamoto [14, 15] for other nomenclature.) Equation (12.3) represents the correlated component of the Y function, which also appears in a subcritical system with Poisson source. The correlation in Eq. (12.3) results from the multiple neutron emissions per fission

Fig. 12.1 Configuration of detector and neutron source in the one-dimensional infinite slab for test calculations

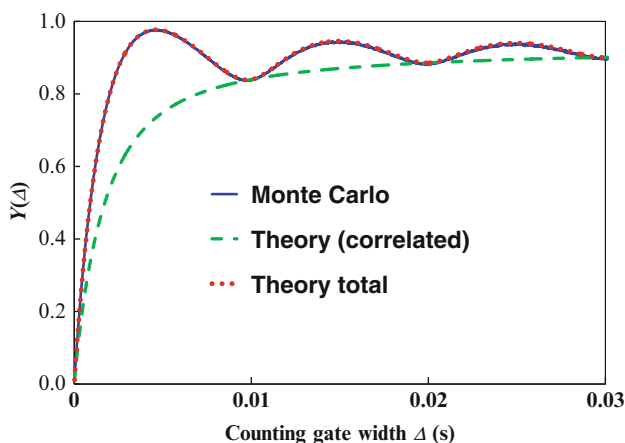
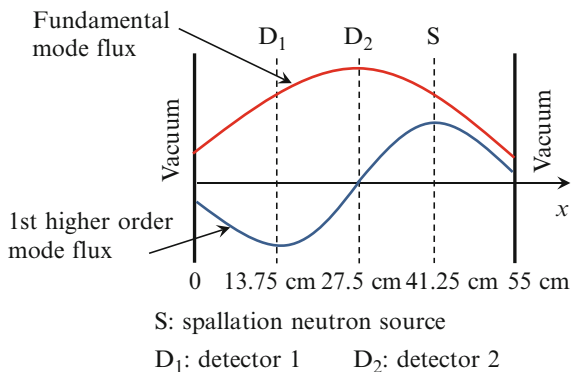


Fig. 12.2 Feynman Y function versus counting gate width by Monte Carlo simulation and theoretical value at the detector 1

reaction. Equation (12.4) represents another correlated component caused by periodically pulsed multiple neutrons. Equation (12.5) represents the uncorrelated component caused by the periodically pulsed spallation neutron source.

A numerical example is considered for a one-dimensional slab with infinite height. The thickness of the slab is $H = 55$ cm. The vacuum boundary conditions are imposed on both ends of the slab. The spallation neutron source and neutron detectors are allocated as shown in Fig. 12.1. This chapter considers a one-energy-group problem. The constants used for the numerical example are $\Sigma_t = 0.28 \text{ cm}^{-1}$, $\Sigma_f = 0.049 \text{ cm}^{-1}$, $\Sigma_c = 0.05 \text{ cm}^{-1}$, $v = 2,200 \text{ m/s}$, $\nu = 2$, and $q = 60$, $T = 0.01$ s (100 Hz). This system is sufficiently subcritical and $k_{\text{eff}} = 0.95865 \pm 0.00002$, which is obtained by a Monte Carlo criticality calculation (it is referred to as “large subcritical system” hereinafter). The Feynman Y function versus counting gate width Δ at the position of the detector 1 in Fig. 12.1 is calculated with a Monte Carlo simulation of the Feynman- α method. The simulation result at detector 1 is shown in Fig. 12.2 as “Monte Carlo.” In Fig. 12.2, “Theory (correlated)” shows a

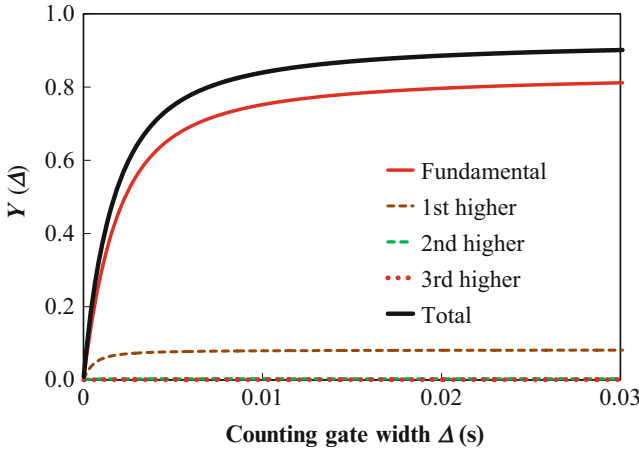


Fig. 12.3 Mode components of the correlated component in the Feynman Y function

theoretical value of the sum of $Y_C(\Delta)$ and $Y_{CS}(\Delta)$ calculated with Eqs. (12.3) and (12.4). “Theory total” shows “Theory (correlated)” plus the theoretical value of the uncorrelated component $Y_{UN}(\Delta)$, calculated with Eq. (12.5). The neutron flux and α_m , which are needed to calculate the theoretical values of Eqs. (12.3), (12.4), and (12.5), are calculated with the Monte Carlo method up to the third-order mode [16]. Beyond the third order, those are approximated with the diffusion theory:

$$\alpha_m = v(\Sigma_f + \Sigma_c + DB_m^2 - \nu\Sigma_f), m \geq 4 \tag{12.6}$$

$$\psi_m(x) = \sqrt{\frac{2v}{H + 2d}} \sin B_m(x + d), m \geq 4 \tag{12.7}$$

$$B_m = \frac{(m + 1)\pi}{H + 2d}. \tag{12.8}$$

where $d = \text{extrapolated length} (=0.7104/\Sigma_t)$. The summation in Eqs. (12.3), (12.4), and (12.5) is taken up to the 250th mode. As shown in Fig. 12.2, there is good agreement between the Monte Carlo simulation and the theory, which shows verification of the theoretical formula of Eq. (12.2). Using Eqs. (12.3), (12.4), and (12.5), the Feynman Y function is decomposed into mode components. Figures 12.3 and 12.4 show the mode components of the correlated component and of the uncorrelated component, respectively. In these figures, each mode component includes the cross terms with the lower-order mode components. For example, “1st higher” includes the cross terms between the fundamental mode and the first higher-order mode as well as the first higher-order mode itself. Figure 12.1 shows that detector 1 is located at the bottom of the first higher-order mode. Thus, the first higher-order mode has a significant effect on the Feynman Y function of detector 1. Especially, the higher-order mode is more remarkable in the uncorrelated component, as shown in Fig. 12.4.

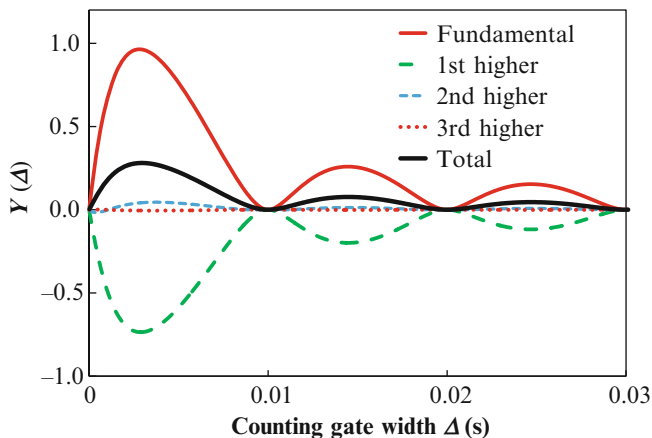
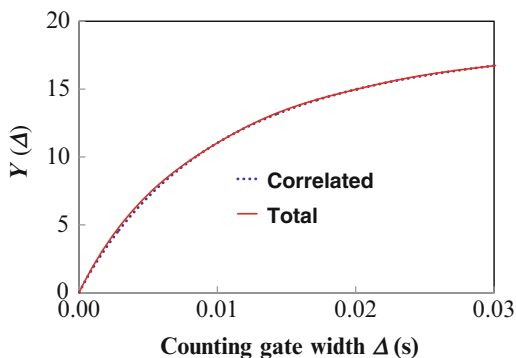


Fig. 12.4 Mode components of the uncorrelated component in the Feynman Y function

Fig. 12.5 Feynman Y function in the nearly critical system



For a “nearly critical system” ($k_{\text{eff}} = 0.99242 \pm 0.00002$), the Feynman Y function is calculated using Eq. (12.2). The constants used for the nearly critical system are $\Sigma_t = 0.2834 \text{ cm}^{-1}$, $\Sigma_f = 0.0524 \text{ cm}^{-1}$, $\Sigma_c = 0.05 \text{ cm}^{-1}$, $\nu = 2$, 200 m/s , $\nu = 2$, $q = 60$, and $T = 0.01 \text{ s}$ (100 Hz). The Feynman Y function versus the counting gate width is shown in Fig. 12.5. “Total” in Fig. 12.5 shows the sum of the correlated and uncorrelated components. As shown in Fig. 12.5, the uncorrelated component is very minor in the nearly critical system. Thus, the Feynman Y function is almost the same as the correlated component. The higher modes are negligibly small in the correlated component in the nearly critical system. Thus, the accurately approximated fundamental mode α can be obtained by fitting the Feynman Y function to the conventional formula, Eq. (12.1). On the other hand, if the subcriticality is not small enough, the uncorrelated component and higher-order modes have significant effects on the Feynman Y function. Therefore, obtaining a fundamental mode α would become difficult by simply fitting the Feynman Y function to Eq. (12.1). The Feynman- α method is not necessarily a suitable method as a subcriticality measurement technique.

12.3 Theory of Power Spectral Density in ADS

Another subcriticality measurement technique is the power spectral density method. This chapter focuses on the cross-power spectral density (CPSD), which is the Fourier transformation of a cross-correlation function between two neutron detector signals. In an infinite and homogeneous subcritical system where the energy and spatial dependence of the neutron is neglected, the CPSD is simply expressed as a function of frequency:

$$\text{CPSD}(\omega) \propto 1/(\omega^2 + \alpha_0^2), \quad (12.9)$$

where ω = angular frequency. The CPSD in an ADS where the energy and spatial dependence is considered, however, is much more involved as

$$\text{CPSD}(\omega) = \text{CPSD}_C(\omega) + \text{CPSD}_{\text{UN}}(\omega) + \text{CPSD}_{\text{CS}}(\omega), \quad (12.10)$$

$$\begin{aligned} \text{CPSD}_C(\omega) = & \sum_{\ell=0}^{\infty} \sum_{m=0}^{\infty} \sum_{n=0}^{\infty} \frac{S_{\ell} F_{\ell \rightarrow mn} D_{1,m} D_{2,n}}{\alpha_{\ell} (\alpha_m + \alpha_n) (\alpha_n + i\omega)} \\ & + \sum_{\ell=0}^{\infty} \sum_{m=0}^{\infty} \sum_{n=0}^{\infty} \frac{S_{\ell} F_{\ell \rightarrow mn} D_{2,m} D_{1,n}}{\alpha_{\ell} (\alpha_m + \alpha_n) (\alpha_n - i\omega)}, \end{aligned} \quad (12.11)$$

$$\text{CPSD}_{\text{UN}}(\omega) = \frac{2\pi q^2}{T^2} \sum_{n=0}^{\infty} \sum_{\ell=0}^{\infty} \sum_{m=-\infty}^{\infty} D_{1,n} D_{2,\ell} \Psi_n^* \Psi_{\ell}^* \frac{\delta(\omega - \omega_m)}{(\alpha_n - i\omega_m)(\alpha_{\ell} + i\omega_m)}, \quad (12.12)$$

$$\begin{aligned} \text{CPSD}_{\text{CS}}(\omega) = & -\frac{q}{T} \sum_{n=0}^{\infty} \sum_{\ell=0}^{\infty} D_{1,n} D_{2,\ell} \Psi_n^* \Psi_{\ell}^* \frac{1}{\alpha_n + \alpha_{\ell}} \cdot \frac{1}{\alpha_{\ell} + i\omega} \\ & -\frac{q}{T} \sum_{n=0}^{\infty} \sum_{\ell=0}^{\infty} D_{2,n} D_{1,\ell} \Psi_n^* \Psi_{\ell}^* \frac{1}{\alpha_n + \alpha_{\ell}} \cdot \frac{1}{\alpha_{\ell} - i\omega}, \end{aligned} \quad (12.13)$$

where $i = \sqrt{-1}$, $\omega_m = 2\pi m/T$, and the subscripts C , UN , and CS have the same meanings as in the previous section. For the two systems in the previous section (large subcritical system and nearly critical system), Monte Carlo simulations were performed to obtain CPSDs between detectors 1 and 2 in Fig. 12.1. In the simulations, the pulse period is $T = 0.05$ s (20 Hz). The simulation result for the nearly critical system is compared with the theoretical one in Fig. 12.6. The results of the large subcritical system are shown by Yamamoto [15]. The theoretical results agree well with the Monte Carlo simulations. The uncorrelated component, $\text{CPSD}_{\text{UN}}(\omega)$, emerges only at the integer multiples of the pulse frequency as the Delta-function-like peaks. Thus, either of the correlated and uncorrelated components can be easily discriminated from the CPSD. Using Eq. (12.12), the uncorrelated and correlated components of the CPSD in the nearly critical system is decomposed into the mode components, shown in Figs. 12.7 and 12.8, respectively. In the correlated

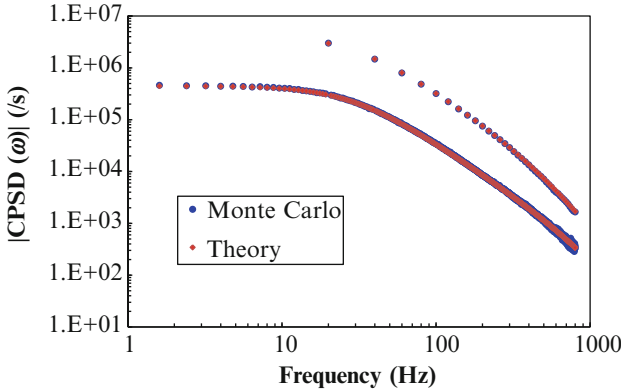


Fig. 12.6 Amplitude of cross-power spectral density (CPSD) in the nearly critical system by Monte Carlo simulation and theoretical value

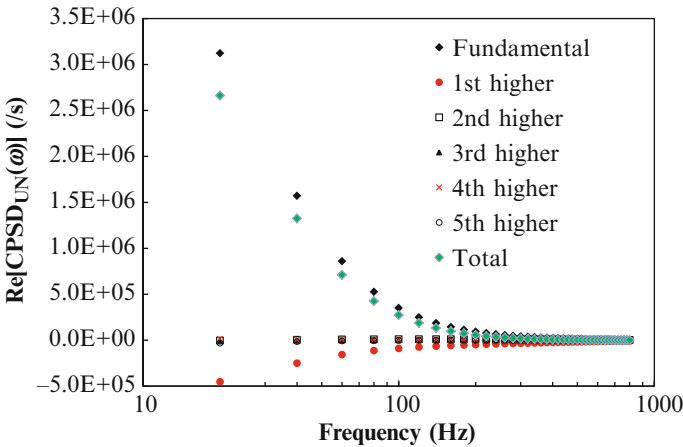


Fig. 12.7 Mode components of the uncorrelated component in the CPSD in the nearly critical system (real part)

component, the higher-order modes are negligibly small, and almost the whole of the CPSD is made up of the fundamental mode. The same condition holds for the large subcritical system. The higher-order mode effect in the correlated component is minor even in the large subcritical system. In the uncorrelated component, the higher-order mode effect is significant even in the nearly critical system. In the large subcritical system, the higher-order mode effect is much more significant. Thus, fitting the uncorrelated component to Eq. (12.9) yields an inaccurate α value unless the system is nearly critical. For example, in the large subcritical system we obtain $\alpha = 789 \text{ (s}^{-1}\text{)}$ for the true fundamental mode α value of $940 \text{ (s}^{-1}\text{)}$ [15] from the uncorrelated component. On the other hand, we obtain $\alpha = 900 \text{ (s}^{-1}\text{)}$ from the

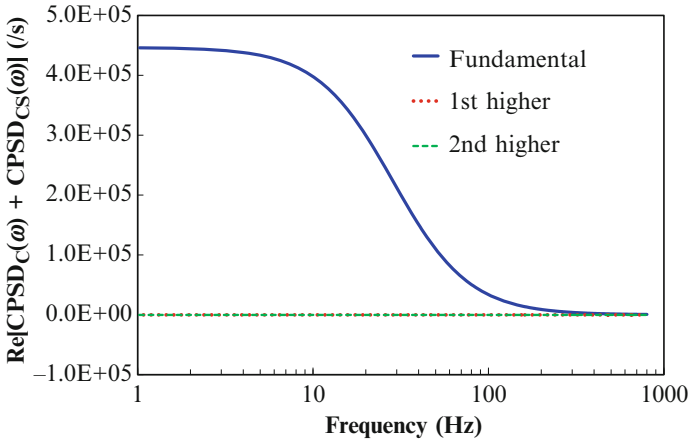


Fig. 12.8 Mode components of the correlated component in the CPSD in the nearly critical system (real part)

correlated component. In the nearly critical system, we obtain $\alpha = 172 \text{ (s}^{-1}\text{)}$ and $178 \text{ (s}^{-1}\text{)}$ from the uncorrelated and correlated component, respectively, for the true fundamental mode α value of $179 \text{ (s}^{-1}\text{)}$ [15].

12.4 Conclusions

In a subcriticality measurement for an ADS, the Feynman Y function in general appears as the sum of the correlated and uncorrelated components. The higher-mode effect in the correlated component is less significant than in the uncorrelated component. Thus, a relatively good approximation of the true fundamental mode α can be obtained by using the correlated component. However, it is not necessarily easy to separate the correlated component from the measured Feynman Y function. Considering the difficulty of separating the correlated component, the Feynman- α method is not always suitable as a subcriticality measurement technique for ADSs. In an ADS that is nearly critical, the uncorrelated component is very minor. Thus, by fitting the measured Feynman Y function to the correlated component, the fundamental mode α can be accurately estimated.

In a subcriticality measurement using the power spectral density method, the uncorrelated component emerges at the integer multiples of the pulse frequency as delta-function-like peaks. Thus, the uncorrelated component can be easily discriminated from the correlated component. The correlated component is less contaminated by the higher-order modes. An approximate fundamental mode α can be obtained by fitting the Feynman Y function to the correlated component of the power spectral density. The use of the uncorrelated component is not always recommended, because the higher-order modes are more significant in the uncorrelated component.

Open Access This chapter is distributed under the terms of the Creative Commons Attribution Noncommercial License, which permits any noncommercial use, distribution, and reproduction in any medium, provided the original author(s) and source are credited.

References

1. Pázsit I, Ceder M, Kuang Z (2004) Theory and analysis of the Feynman-alpha method for deterministically and randomly pulsed neutron sources. *Nucl Sci Eng* 148:67–78
2. Pázsit I, Kitamura Y, Wright J, Misawa T (2005) Calculation of the pulsed Feynman-alpha formulae and their experimental verification. *Ann Nucl Energy* 32:986–1007
3. Kitamura Y, Taguchi K, Misawa T, Pázsit I, Yamamoto A, Yamane Y, Ichihara C, Nakamura H, Oigawa H (2006) Calculation of the stochastic pulsed Rossi-alpha formula and its experimental verification. *Prog Nucl Energy* 48:37–50
4. Muñoz-Cobo JL, Peña J, González E (2008) Rossi- α and Feynman Y functions for non-Poissonian pulsed sources of neutrons in the stochastic pulsing method: application to subcriticality monitoring in ADS and comparison with the results of Poissonian pulsed neutron sources. *Ann Nucl Energy* 35:2375–2386
5. Muñoz-Cobo JL, Rugama Y, Valentine TE, Mihalczó JT, Perez RB (2001) Subcritical reactivity monitoring in accelerator-driven systems. *Ann Nucl Energy* 28:1519–1547
6. Rugama Y, Muñoz-Cobo JL, Valentine TE (2002) Modal influence of the detector location for the noise calculation of the ADS. *Ann Nucl Energy* 29:215–234
7. Ballester D, Muñoz-Cobo JL (2006) The pulsing CPSD method for subcritical assemblies driven by spontaneous and pulsed sources. *Ann Nucl Energy* 33:281–288
8. Degweker SB, Rana YS (2007) Reactor noise in accelerator driven systems: II. *Ann Nucl Energy* 34:463–482
9. Sakon A, Hashimoto K, Sugiyama W, Taninaka H, Pyeon CH, Sano T, Misawa T, Unesaki H, Ohsawa T (2013) Power spectral analyses for a thermal subcritical reactor system driven by a pulsed 14 MeV neutron source. *J Nucl Sci Technol* 50:481–492
10. Endo T, Yamane Y, Yamamoto A (2006) Space and energy dependent theoretical formula for the third order neutron correlation technique. *Ann Nucl Energy* 33:521–537
11. Muñoz-Cobo JL, Bergöf C, Peña J, González E, Villamarín D, Bournos V (2011) Feynman- α and Rossi- α formulas with spatial and modal effects. *Ann Nucl Energy* 38:590–600
12. Yamamoto T (2011) Higher order mode analyses in Feynman- α method. *Ann Nucl Energy* 38:1231–1237
13. Yamamoto T (2013) Energy-higher order mode analyses in Feynman- α method. *Ann Nucl Energy* 57:84–91
14. Yamamoto T (2014) Frequency domain Monte Carlo simulation method for cross power spectral density driven by periodically pulsed neutron source using complex-valued weight Monte Carlo. *Ann Nucl Energy* 64:711–720
15. Yamamoto T (2014) Higher order mode analyses of power spectral density and Feynman- α method in accelerator driven system with periodically pulsed spallation neutron source. *Ann Nucl Energy* 66:63–73
16. Yamamoto T (2011) Higher order α mode eigenvalue calculation by Monte Carlo power iteration. *Prog Nucl Sci Technol* 2:826–835